Analysis of Glycerol-^{3}H Transport in the Frog Oocyte by Extractive and Radioautographic Techniques

SAMUEL B. HOROWITZ and I. ROBERT FENICHEL

From the Cellular Biophysics Laboratory, Albert Einstein Medical Center, Philadelphia, Pennsylvania 19141

ABSTRACT The efflux of glycerol-^{3}H from mature *R. pipiens* oocytes was studied by extractive analysis and by quantitative radioautography using techniques suitable for diffusible solutes. Extractive analysis was used to determine the total cellular concentration of tracer, and radioautography, regional intracellular concentrations, at equilibrium and as a function of efflux time, t_E. The efflux was resolvable into four kinetic fractions: cytoplasmic fast and slow fractions, and nuclear fast and slow fractions. The fast fractions represent freely diffusible glycerol in the two compartments; the solvent space accessible to glycerol is unity in the nucleus (germinal vesicle), but only 0.73 in the cytoplasm. The efflux of both fast fractions from the cell is determined by the permeability of the cortical membrane, with neither the nuclear membrane nor diffusion in the cytoplasm detectably slowing the flux. The permeability at 13.6°C is 2.2×10^{-5} cm/sec. The slow fractions leave the cell at about one-tenth the rate of the fast; the interpretation is that these fractions represent glycerol bound to impermeant cellular constituents. The size of these constituents is below the radioautographic resolution; in the cytoplasm, they appear not to be the yolk platelets. The extent of binding is about fourfold greater, per milliliter of compartment water, in the cytoplasm than in the germinal vesicle.

INTRODUCTION

Transport processes are generally monitored by following the flux of a tracer into, out of, or across a whole cell or a multicellular preparation. This technique has two obvious limitations. First, if complex or "multicompartmental" flux kinetics are found, there is no rigorous way to identify the origins of the contributing terms. Second, there is no way to monitor separately the local transport process in intracellular inclusions of specific interest, such as the nucleus. These limitations can be partly alleviated by studying transport in isolated subcellular preparations, but one is then faced with problems of purification and deterioration, which cannot be controlled by reference to behavior *in situ*.

Methods are needed for determination of concentrations of permeant solutes locally within the cell during transport. A promising technique for this type of analysis is radioautography under conditions in which the cell is kept at sufficiently low temperature to prevent solute redistribution by diffusion from the time of original freezing and sectioning to the completion of the radioautograph. Several such techniques have appeared in recent years (1–3).

This paper reports experiments in which the flux of glycerol-2-^{3}H from frog oocytes into a medium free of tracer was followed by two methods: analysis of total tracer content of the oocyte by extraction and liquid scintillation counting, and analysis of radioautographs of frozen sections of the oocyte made at −73°C.

The frog oocyte is a nearly ideal cell for this type of analysis, for both physiological and technical reasons. With respect to the former, the oocyte is quite typical in a number of membrane properties (e.g., a K^+-sensitive membrane potential (4), selective Na^+ exclusion (5–7), and Na^+-dependent uphill amino acid transport (6, 8), while, on the other hand, multicompartment transport kinetics have been repeatedly observed (5, 6, 9–11). Furthermore, the large size of the oocyte's major inclusion, the germinal vesicle (nucleus), makes it of specific interest with respect to the permeability of nuclear membranes. Technically, the large size, regular shape, and ease of isolation of the oocyte reduce the experimental difficulties involved with extracellular tracer in extractive procedures, as well as greatly mitigating the resolution problems associated with radioautography.

We have obtained good radioautographic quantitation and resolution. This has permitted information to be obtained about the localization of solute, the relative permeabilities of nuclear and cortical membranes, and the origin of multicompartmental kinetics in this cell. Further improvement of the technique itself appears feasible, and is discussed.

MATERIALS

Oocytes Mature ovarian oocytes were isolated from *R. pipiens* obtained from a New Jersey dealer during the months of January, March, and December. No significant differences were seen in oocytes obtained during these months. The procedure for oocyte isolation, trimming, selection, and handling is given by Abelson and Duryee (5). The average weight of an oocyte was 2.80 ± 0.21 mg, (21 oocytes) of which 48.9% was dry weight. Taking a specific gravity of 1.14 (6) the average volume was 2.45×10^{-3} cm^3. The average volume based on the dimensions of histological sections was $2.28 \pm 0.27 \times 10^{-3}$ cm^3 (15 oocytes). The difference could be accounted for by a 2.2% decrease in radius due to shrinkage when the sections were dehydrated. The oocytes were stage Y_5 of Kemp (12). The follicular envelopes were trimmed flush. Average nuclear (germinal vesicle) volume was 4.75×10^{-5} cm^3, or 2.4% of the cellular volume. The cytoplasm is packed with ovoid yolk platelets which may be as

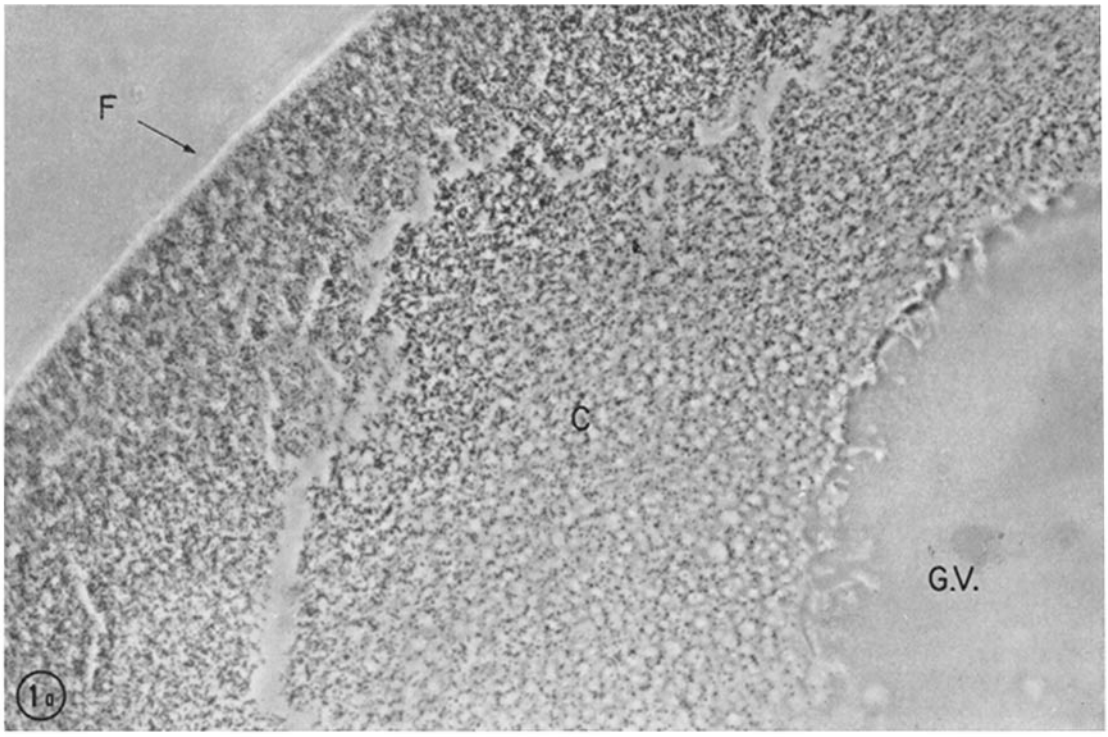

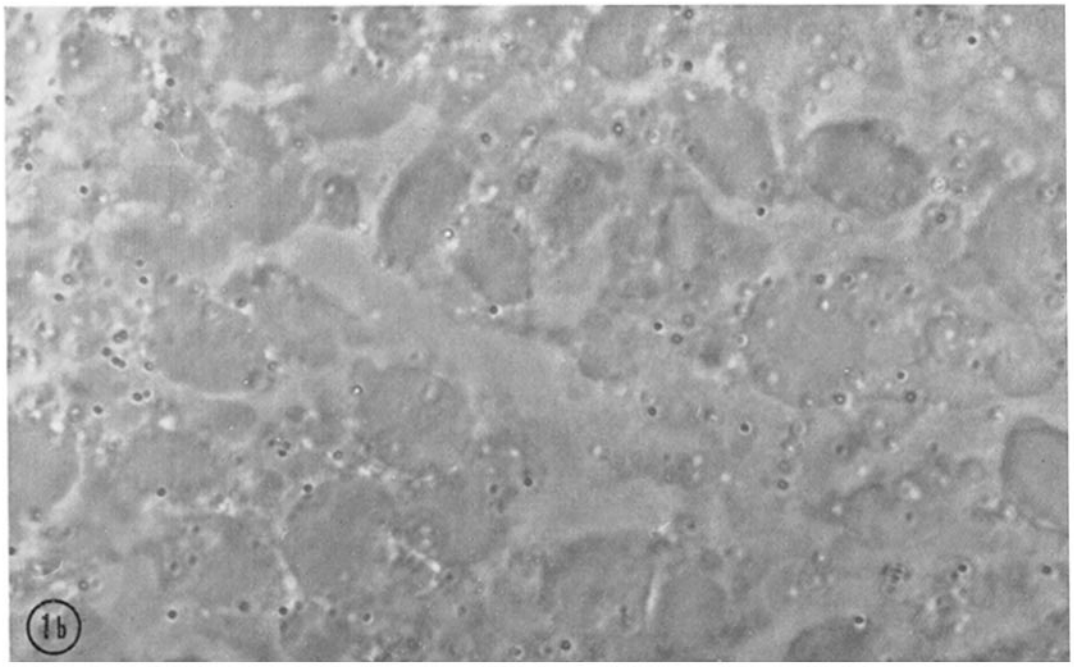

FIGURE 1. Phase contrast photomicrographs of unstained sections of a stage Y_5 oocyte of *R. pipiens*. (*a*) Animal hemisphere at low power; seen are clear germinal vesicle (*G.V.*), densely pigmented inclusion-bearing cytoplasm (*C*), and follicular epithelium (*F*). × 500. (*b*) Vegetal hemisphere at somewhat greater magnification, with large yolk platelets interspersed with ground cytoplasm which bears pigment granules and other inclusions. × 1800.

large as 10 μ × 7 μ in the vegetal hemisphere (Fig. 1 b), and decrease in size as the animal pole is approached. Pigment granules are a conspicuous element in the ground cytoplasm between yolk platelets and are extremely dense in the animal hemisphere (Fig. 1 a). A number of careful descriptions of the fine structure of the frog oocyte are available (13–16).

Solutions Ringer's solution containing glycerol (G-Ringer's) consisted of 2.3 mM glycerol; 24.0 mM glucose; 92.7 mM NaCl; 2.5 mM KCl; 1.0 mM $CaCl_2$; 1.2 mM $MgSO_4$; 17.3 mM $NaHCO_3$; 2.0 mM NaH_2PO_4; 1.2 mM Na_2HPO_4. The pH was 7.2–7.3.

Glycerol-2-^{3}H was obtained from the New England Nuclear Corporation, lot 160-258A, and was used without further purification. Radiochromatographic purity given by the manufacturer was >96%. This was confirmed by paper chromatography in two different solvent systems (see page 708). Ringer's solution containing 2.3 mM radioactive glycerol (G*-Ringer's) was otherwise identical with the above, and had a specific activity of 339 μc/ml. Oocytes to be radioautographed were frozen in either G-Ringer's or G*-Ringer's containing 15% w/v of bovine serum albumin fraction V (Nutritional Biochemical Corporation); these solutions are designated AG-Ringer's and AG*-Ringer's, respectively. They are similar to those used by Kinter and Wilson (3).

Radioautographic Plates Kodak NTB emulsion handled in total darkness or under a Wratten 2 safelight, was melted at 40°C and diluted 1:1 with distilled water at the same temperature, with careful stirring. Thoroughly clean microscope slides (25 × 75 mm) were dipped in the emulsion, wiped clean on one side, drained at an 80° angle, and air-dried over moistened absorbent paper at 20°C for 1½ to 2 hr. The plates were stored at 4°C in a light- and air-tight box containing a packet of Drierite®. Emulsion thickness, determined by weighing, was 1.9 ± 0.2 μ. At least 18 hr before use, the boxes containing the plates were placed into the cryostat to cool.

METHODS

The experimental procedure consisted of (*a*) incubation of oocytes in G*-Ringer's, (*b*) washout in G-Ringer's, and (*c*) sampling the oocytes at various times by extraction and scintillation counting or by radioautography.

Incubation All incubation and efflux procedures were performed at 13.6°C. About 30–50 oocytes dissected in G-Ringer's were transferred to a 1 ml vial, the supernatant carefully removed, 0.3 ml of G*-Ringer's added, and the tube permitted to stand with occasional shaking for 8 min. The G*-Ringer was removed and replaced with another 0.3 ml for 5 min. Following the removal of this second G*-Ringer's rinse, 1.0 ml of fresh G*-Ringer's was added and the tube sealed. The two changes of G*-Ringer's were for the purpose of minimizing dilution of the activity to which the oocytes were exposed. Incubation was continued for 18 hr.

Washout Oocytes and incubation (G*-Ringer's) fluid were drawn up into a wide Pasteur pipette and the oocytes permitted to settle in the pipette. The oocytes were discharged into a 15 cm × 0.7 cm glass column containing G-Ringer's (time of

efflux, t_E, is measured from this point) through which they dropped into 250 ml of G-Ringer's in a flask. The contents of the column and 230 ml of the G-Ringer in the flask were discarded. The oocytes were washed with 150 ml of solution into 1300 ml of G-Ringer's in a 5000 ml beaker, the final washout taking place in 1470 ml of solution. The elapsed time at this point was about 15 sec. The oocytes were stirred at a rapid rate by continuous swirling of the beaker. Oocytes were removed from the washout solution at intervals, alternate oocytes being taken for extraction and scintillation counting, and for radioautography. (Oocytes were also taken directly from G*-Ringer's without washing, for equilibrium determination.)

At the beginning and end of a typical experiment, the counting rates of ^3H in the washout fluid were 1.1 and 1.7 $\times$ 10^3 cpm/ml, while in the oocytes these were 46.8 and 3.89 $\times$ 10^6 cpm/ml, respectively; therefore, a dilution factor of 10^3 or greater prevailed at all times, and tracer concentration in the washout fluid was negligible relative to that of the oocytes.

Extraction and Scintillation Counting An oocyte removed from the washout solution was blotted on filter paper, and placed into a vial containing 1.5 ml of G-Ringer's at room temperature. After 24 hr the oocyte was removed from its extraction fluid, blotted, and rapidly weighed on a Cahn electrobalance (Cahn Instrument Co., Paramount, Calif.).

A 1.0 ml aliquot of the extraction fluid was pipetted into a 22 ml counting vial with 20 ml of Bray's solution (17) and counted in a Packard 3214 liquid scintillation counter at 2°C. The standard error of the count was kept below 0.5%. Counting efficiency was determined from the counting rate of an aliquot of G*-Ringer's diluted with G-Ringer's.

The residual activity in the oocyte after this extraction procedure was determined by heating in distilled water at 100°C for 1 hr, following which no activity could be detected in oocytes dissolved in 0.2 M KOH and counted directly. The residual was found to be 3.8 $\pm$ 0.2% of that initially in the cell. The total activity in the oocytes, including this residual, is expressed in microcuries per gram of oocyte, and plotted semilogarithmically against t_E.

In addition to this washout procedure, which extended for about 12,000 sec, oocytes were allowed to wash out for 24 hr at 13.6°C and their remaining activity assessed directly by extraction at 100°C.

Chromatography After incubation and at various times during washout, the identity of labeled material in the washout fluid and that remaining in the cell was examined by chromatography.

To determine the identity of material as it washes out from the oocyte, the following procedure was followed. Oocytes were incubated and washout begun in a large volume in the standard manner. When a collection was desired, an oocyte was transferred to a small volume of washout fluid (0.15 ml per oocyte) and washout continued to the end of the collection period. The use of a small volume was necessary to obtain sufficient activity for chromatography. Aliquots of the washout fluid were used directly for chromatography.

The identity of material within the oocyte at various times was examined as follows. An oocyte taken directly from the incubation medium or taken after a period of

washout was blotted and placed into 1.5 ml of distilled water in an ampoule. The ampoule was sealed and heated at 100°C for 1 hr. The solution was concentrated by freeze drying and 10–40 μl aliquots used for chromatography.

Ascending paper chromatography on Whatman No. 1 paper was employed. Solvents were: methanol: ammonium hydroxide (sp gr 0.896): water, 6:1:3 by volume (18); and pyridine: *n*-butanol: water, 3:6:1 by volume (19). Chromatograms were scanned in a Packard Model 7200 Radiochromatogram scanner.

RADIOAUTOGRAPHY The radioautographic method used is essentially a modification of the "sandwich" technique of Kinter et al. (3, 20).

Freezing Aside from the rapidity of freezing, it is important that the oocyte be mounted in a medium that will permit cutting without extensive distortion and without the egg pulling out of its block. Furthermore, the frozen oocyte must be mounted for sectioning without an excessive rise in temperature.

The narrow end of a No. 5 gelatin capsule (0.45 cm × 1.0 cm) was filled with AG-Ringer's or AG*-Ringer's (for oocytes directly from the incubation medium). The capsule was held in a close-fitting hole in an aluminum block packed in ice. The oocyte to be frozen was drawn into a Pasteur pipette and permitted to settle to the tip of the pipette. It was then extruded with a drop of solution onto the surface of the protein solution in the capsule. The oocyte sank rapidly through the protein solution to the bottom of the capsule leaving the less dense Ringer solution behind. The capsule was grasped with a fine forceps and plunged into a beaker of dichlorodifluoromethane cooled to −160°C with liquid nitrogen. The frozen capsule was stored in liquid nitrogen until required for sectioning. The elapsed time from removal of the oocyte from the washout solution was about 20 sec.

Sectioning and Tissue-Emulsion Contact The capsule containing the oocyte was trimmed of its gelatin coat at dry ice temperature and mounted on the microtome using LKB specimen chuck Model 4820B. Sectioning and contact procedures were carried out in a Lipshaw Cryotome Model 1500, fitted with a Plexiglas® cover containing entrance ports to facilitate manipulation. Sectioning and contact in early experiments were done at −17°C; later experiments (all those reported herein) were performed at −30°C. While the ease of cutting and quality of sections were better at −17°C, radioautographic resolution of diffusible substances substantially improved at the lower temperature. The lower temperature was maintained by packing dry ice in the cryostat.

Sections were cut at 20 μ, which is infinitely thick in respect to the self-absorption of tritium β-particles. An antiroll device was found indispensable. Early in the study the Lipshaw device was used; later the device of Coons et al. (21)[1] was installed. Sections were transferred with a needle point to a Teflon-coated slide (prepared by spraying Fluoroglide® aerosol (Chemplast, Inc., Wayne, N.J.) on 25 × 75 mm microscope slides). Under a safelight an emulsion-coated slide was placed, emulsion downward, on the sections to form a sandwich: slide, Teflon, sections, emulsion, slide. The sandwich was clamped with two spring clips and placed into a light-tight box

[1] Obtained from Edward G. Dixon, Jamesville, N.Y. 13078.

precooled in dry ice. Boxes were replaced in dry ice until stored at −73°C in a Virtis two-stage refrigerator. Exposure was for 18 to 420 hr at −73°C.

20 μ sections of a polymer standard (22), poly(butyl-^{3}H) methacrylate, of activity 441 μc/g, were cut and mounted in the same way.

Development, Mounting, and Bleaching Exposure was terminated by separating the sandwich at room temperature. The sections adhered to the emulsion throughout the entire subsequent procedure. The radioautographic image was developed at 20°C for 6 min in Kodak D19, followed by 10 sec in 1% acetic acid stop bath and 5 min in Kodak Rapid Fix. The radioautographs were washed for 5 min in running water and then 1 min in distilled water. The preparation was dehydrated in graded alcohols, cleared in xylol, and mounted under a cover slip.

The radioautograph at this point was suitable for grain counting in the nuclear and extracellular material, as well as for determining the orientation and dimensions of the sections. However, the high concentration of pigment granules in the cytoplasm, especially in the animal hemisphere and cortex, made accurate grain counting in these areas impossible (see Fig. 1). Since the need for accurate localization of grains made it undesirable to remove the section, a procedure for bleaching the pigment was sought. It was found that treatment at 0°C in 30% hydrogen peroxide (Merck Superoxol®) for 18 to 42 hr (depending on the density of pigment) lowered pigment granule interference to workable levels while having no adverse influence on the emulsion, adhesion of the sections, or grain density. The radioautographs were therefore rehydrated by passage through xylol and graded alcohols, bleached in this manner, and remounted.

Quantitative Analysis of Radioautographs Grain counting was done at a magnification of 1200 in phase contrast, using a Whipple-Hausser type eyepiece micrometer. The grains appeared essentially in a single plane of focus as bright refractile spots beneath the section.

1. Resolution. Experimentally determined grain density profiles at the edges of three types of sources, all sectioned and exposed as described above, are shown in Fig. 2.

Fig. 2 a is for the nondiffusible tritium source, poly(butyl-^{3}H) methacrylate. The resolution, taken as the distance at a source edge in which the grain density falls by 50%, in this case is limited, not by the radioautograph but by the statistics of counting and the measuring system utilized (cf. Hill, 23). The smallest area over which it was practical to make differential counts was a square 6.9 μ on a side. Resolution of a nondiffusible source may be taken as less than one-half this length.

Resolution of a diffusible source was determined at the edge of a section cut from AG*-Ringer's (Fig. 2 b); it is poorer than that of the nondiffusible source, about 14 μ. The resolution in radioautographs of the oocyte proper can be estimated by assuming that the tritium concentration discontinuity at the oocyte surface (see Results) is sharp, and by determining the grain density profile through the discontinuity. An example is provided in Fig. 2 c which shows that resolution at the cell boundary is also about 14 μ. These results suggest that some solute redistribution takes place during the period of radioautographic contact despite the precautions taken. However, this

redistribution is small in respect to the dimensions of the oocyte with which we will be concerned and can be properly ignored.

Apparent resolutions better than 14 μ may be interpreted as arising from activity whose redistribution is restricted either by adsorption to a nondiffusible matrix, or by local inhomogeneities of solubility.

2. Calibration and Multiple Hit Correction. Using discs of poly(butyl-^{3}H) methacrylate a calibration curve was prepared relating grain density to the tritium activity, A, of a section in millicuries per gram and the radioautographic exposure time, t_A, in hours, in the range 0–40 mc hr/g. As expected, a linear relation was found at low

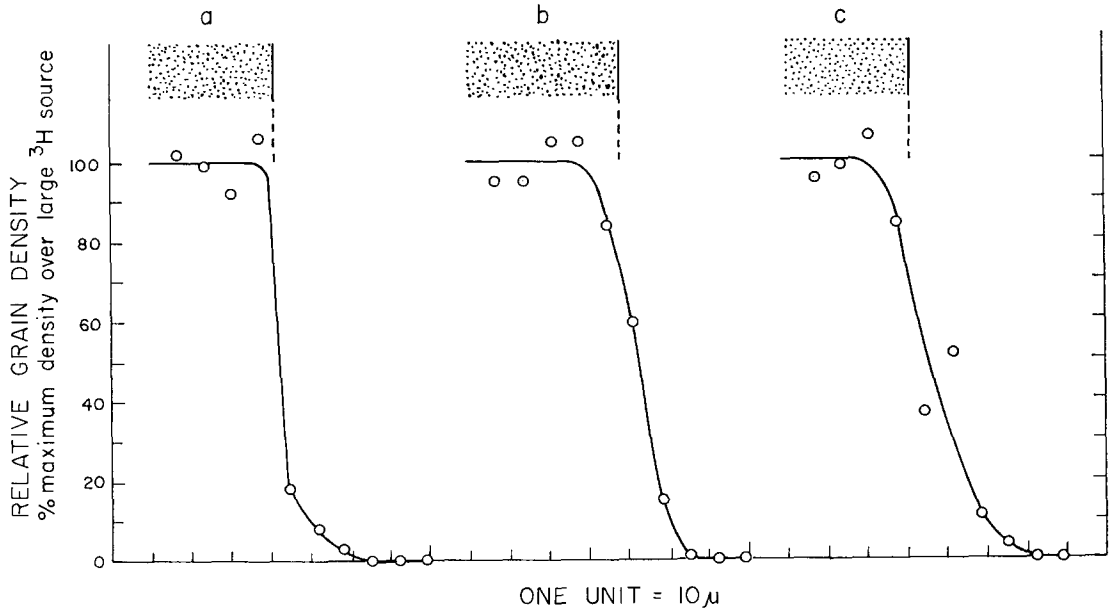

FIGURE 2. Grain density profiles of radioautographs taken at the border of 20 μ sections of ^{3}H sources. See text for procedure. (a) Poly(butyl-^{3}H) methacrylate. (b) Frozen AG*-Ringer's solution. (c) Vegetal hemisphere of oocyte equilibrated in glycerol-^{3}H Ringer's solution, washed out for 260 sec into G-Ringer's, and frozen in AG-Ringer's.

exposure levels (24), though the influence of grain saturation becomes appreciable above 7 mc hr/g. The points in Fig. 3 are experimental, and are described by an equation (the curved line, a, of Fig. 3):

$$\text{grains}/1000\ \mu^2 = 9.91\ At_A - 0.0972\ A^2t_A^2 .$$

All grain densities in oocyte sections, G, have been corrected for multiple hits and are expressed in grains/1000 μ^2/hr. The observed density was corrected by determining the theoretical density on curve b of Fig. 3 corresponding to the observed value on curve 3 a. Conversion of grain density to tritium activity is described in the Results.

3. Artifacts. Though artifacts have not presented a serious problem to the present studies, two types have been observed.

At the border of cells, a thin line of high grain density was occasionally observed, as in Fig. 4 a. These might be interpreted as thin, cortical regions of high activity. However, the line coincides only with part of the circumference of the oocyte and with no particular zone or structural feature. Furthermore, identical lines were commonly seen at the edges of sections of polymerized methacrylate, in which activity is known

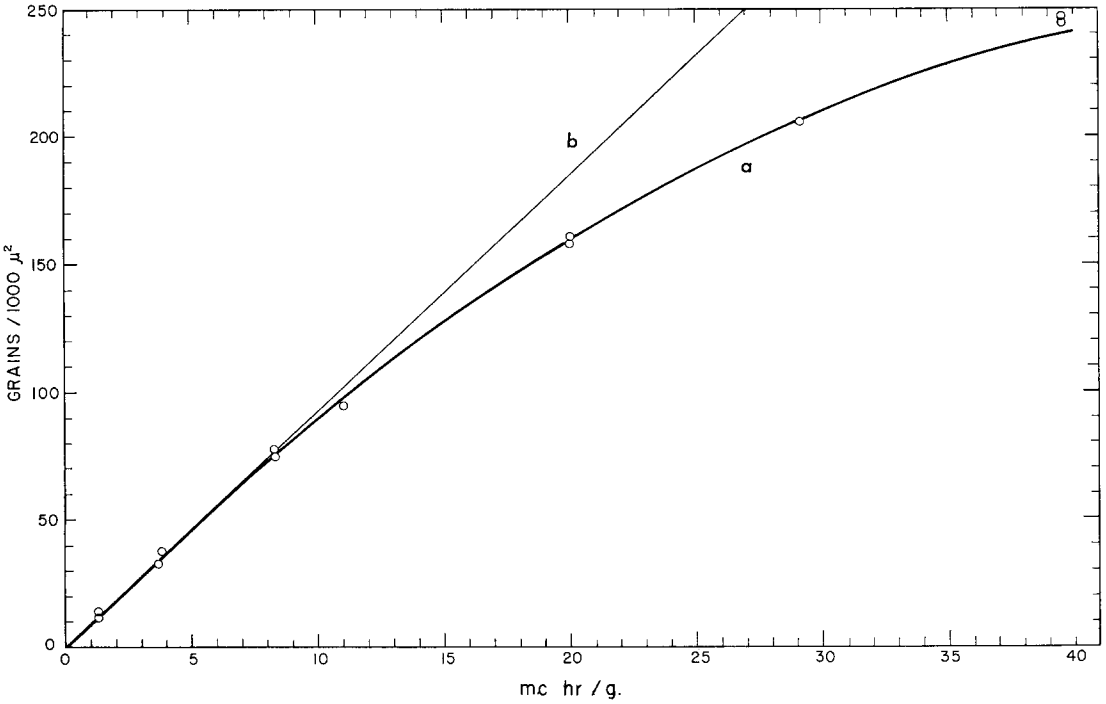

FIGURE 3. Relation between exposure to a tritiated source, poly(butyl-^3H) methacrylate, and grain density in NTB emulsion. Specific activity of the source was 0.441 mc/g; t_A = 2.9 to 89.7 hr; exposure at −73°C. Points are experimental; for lines see text.

to be homogeneously distributed. The lines are probably pressure artifacts (25, 26), a consequence of the clamping procedure used in making section-emulsion contact.

A second artifact is not uncommonly seen in radioautographs beneath nuclei and AG*-Ringer's but not beneath cytoplasm. These are alternate bands of high and low grain counts in locations in which a uniform distribution is expected. Examples of this artifact are shown as Figs. 4 b and c. We tentatively attribute this artifact to the poorer cutting and contact properties of the nucleus and the AG*-Ringer. Frozen, these materials are probably less plastic than cytoplasm because of their higher ice content, and conform less well to the surface of the emulsion, so that they reflect more sensitively nonplanar features in both sections and emulsion surface.

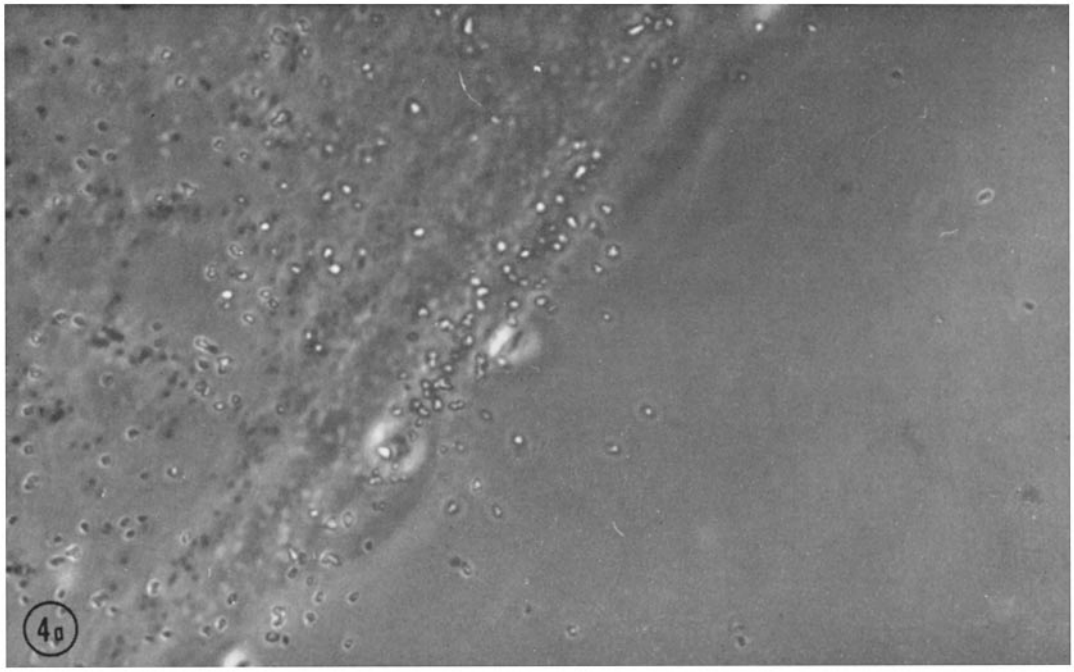

FIGURE 4. Radioautographic artifacts: (*a*) Lines of high grain density at edge of cell. × 1800. (*b*) Alternate bands of high and low density over AG*-Ringer's. × 720. (*c*) Similar bands in portion of a nucleus. × 1150. For additional explanation, see text.

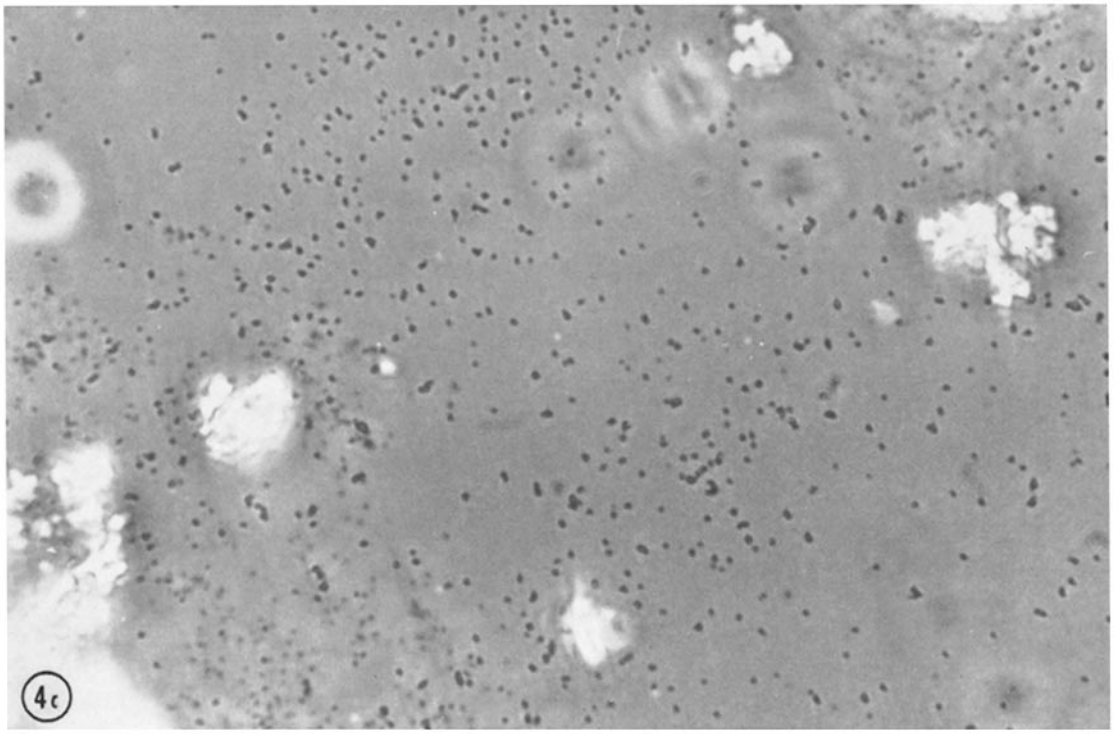

FIGURE 4 *continued*

RESULTS

Analysis by Extraction

The activity in the oocyte after 18 hr of incubation, $\bar{C}(O)$, was 163.1 ± 0.3 μc/g. The time course of efflux of activity is shown in Fig. 5. The points are fitted by the following expression:

$$\bar{C}(t_E) = C_f e^{-k_f t_E} + C_s e^{-k_s t_E} + C_\infty \quad (1)$$

where $\bar{C}(t_E)$ is the activity in the oocyte, in microcuries per gram, after t_E sec of washout; $C_f = 0.779\ \bar{C}(O)$, $C_s = 0.134\ \bar{C}(O)$, $k_f = 7.7 \times 10^{-4}$ sec^{-1}, $k_s = 8.8 \times 10^{-5}$ sec^{-1}, and $C_\infty = 0.053\bar{C}(O)$. These three terms account for all but 3.4% of the activity, which is probably rapidly lost, adherent extracellular material. C_∞ represents the amount of activity remaining in the egg after 24 hr of efflux at 13.6°C. Its rate constant is presumably on the order of a factor of 10 less than k_s.

We designate the first term on the right side of equation 1 as the fast fraction, and the second and third terms together as the slow fraction.

As described in Methods, to determine the chemical identity of the fast and slow fractions, radiochromatograms were prepared of the following: (*a*) whole extracts of oocytes at $t_E = 0$, $t_E = 9000$ sec (by which time only the slow fraction remains in detectable amounts), and $t_E = 89{,}000$ sec; (*b*) washout fluid collected between 9000 and 89,000 sec. In each case all but an insignificant fraction of the activity moved as a single radiochromatographic peak,[2] coinciding with that of a glycerol standard in both pyridine-butanol-water ($R_f = 0.52$) and methanol-ammonia-water ($R_f = 0.82$). The same results were obtained when glycerol-1,3-^{14}C was used in place of glycerol-2-^{3}H. We infer that the fast and slow fractions are chemically unmodified glycerol.[2]

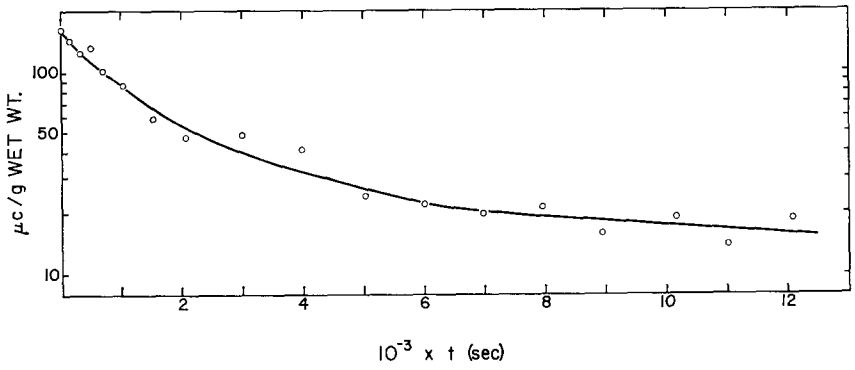

FIGURE 5. Oocyte concentration of glycerol-^{3}H, determined by the extractive method, as a function of efflux time at 13.6°C. Points experimental, solid line fitted.

Radioautography

Representative radioautographs of oocyte sections are shown in Figs. 6–9 and grain density profiles in Figs. 10 and 11. Each profile in Fig. 10 is taken close to the widest point of the oocyte. All sections are somewhat diagonal so that the cell boundary C is in the animal hemisphere while C' is in the vegetal hemisphere. The vertical bar to the right of each profile indicates 1 SE to either side of an ordinate value (the central bar), taken as the square root of the absolute number of grains (less background) counted to establish the value. Generally, points were taken 69 μ apart and each point represents the grain count in 4761 μ^2. When greater resolution was desired, points were taken more closely together. The scale of the ordinate is the same for all profiles.

Fig. 6 shows part of the cytoplasm and the adjacent AG*-Ringer of an

[2] Oocytes in earlier developmental stages phosphorylate glycerol, to give α-glycerol phosphate (data to be published). No glycerol phosphate is detected in the mature oocytes used in this study. The present extraction technique does not hydrolyze glycerol phosphate ((27) and confirmed by us).

In the mature egg, a small amount of tracer remains at the origin of the radiochromatographs. It amounts to less than 4% of the slow fraction or 15% of C_∞. It has not been identified.

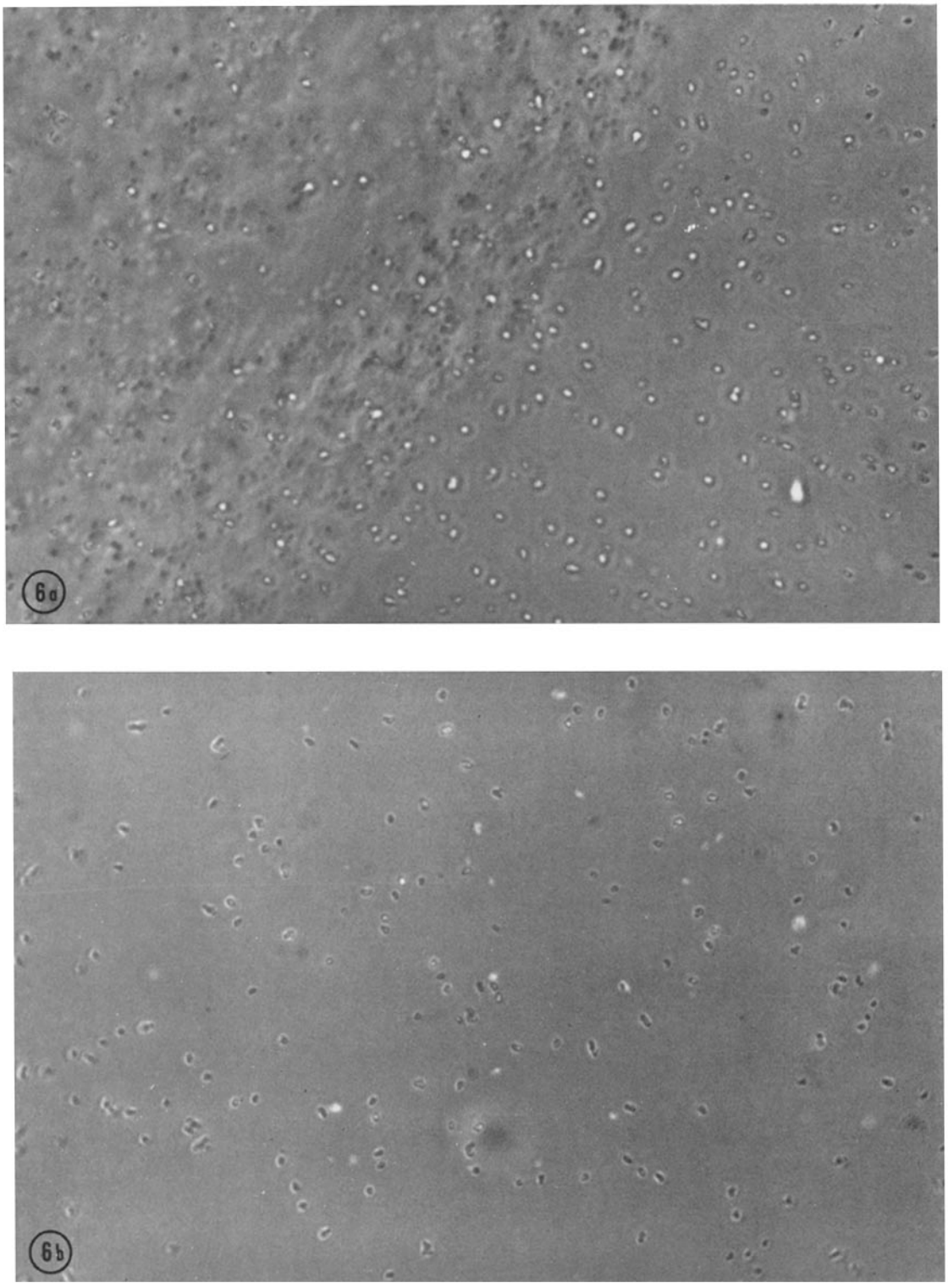

FIGURE 6. Phase contrast views of a radioautograph of an oocyte at equilibrium (t_E = 0) with glycerol-^{3}H Ringer's solution. (*a*) Oocyte–AG*-Ringer's border. (*b*) Vegetal hemisphere cytoplasm, showing characteristic reticulate silver grain pattern. × 1800.

oocyte incubated in G*-Ringer's for 18 hr and then frozen and sectioned in AG*-Ringer's. The grain density profile through the section is shown in Fig. 10 a; within the resolution of the technique, the density is uniform within each phase and there is a sharp discontinuity at the cell surface.

Fig. 7 shows part of the cytoplasm and the adjacent AG-Ringer of an oocyte washed out for 260 sec in G-Ringer's, then frozen and sectioned in AG-Ringer's. Figs. 10 b to 10 e show grain density profiles for oocytes washed out

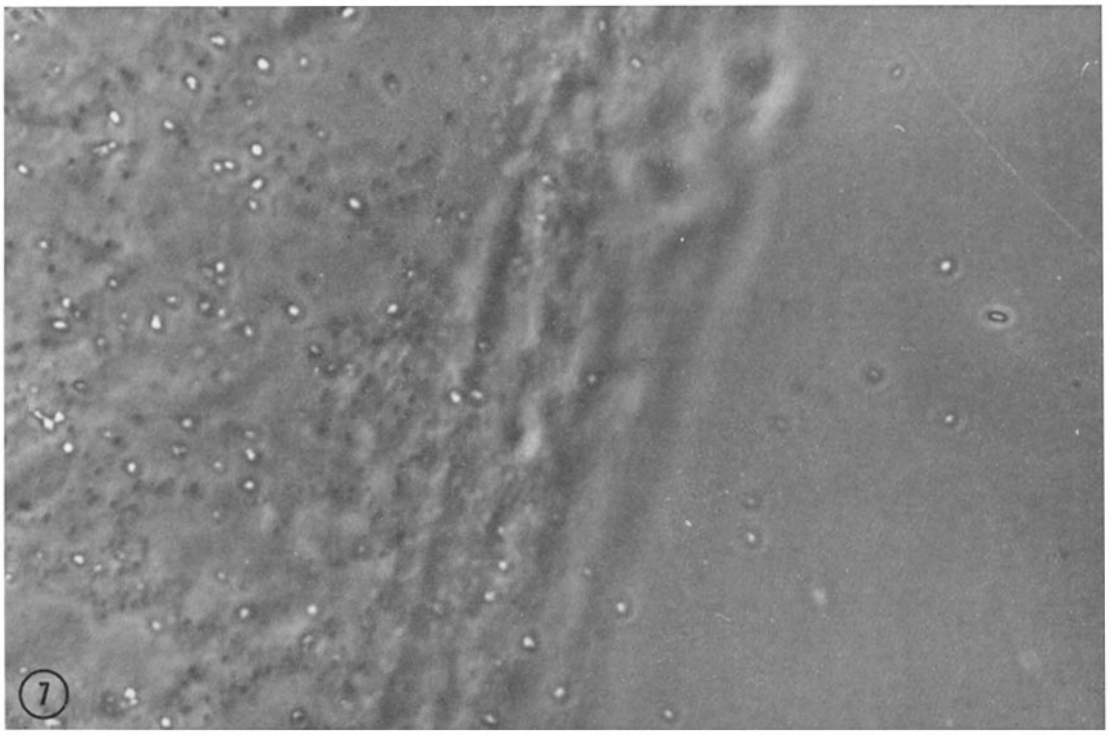

FIGURE 7. Phase contrast view of a radioautograph of the oocyte–AG-Ringer border at t_E = 260 sec. × 1800.

for periods of from 260 to 12,020 sec. Grain density declines during washout; at all times of washout the grain density is uniform within the cytoplasm and is sharply discontinuous at the oocyte border.

In Figs. 8 and 9 are shown radioautographs of part of the germinal vesicle and adjacent cytoplasm of oocytes which have been washed out for 260 and 8890 sec, respectively, and frozen and sectioned in AG-Ringer's. Fig. 11 shows profiles through the germinal vesicle and surrounding animal hemisphere cytoplasm at equilibrium (Fig. 11 a) and after washout for from 260 to 12,020 sec (Figs. 11 b to 11 e).

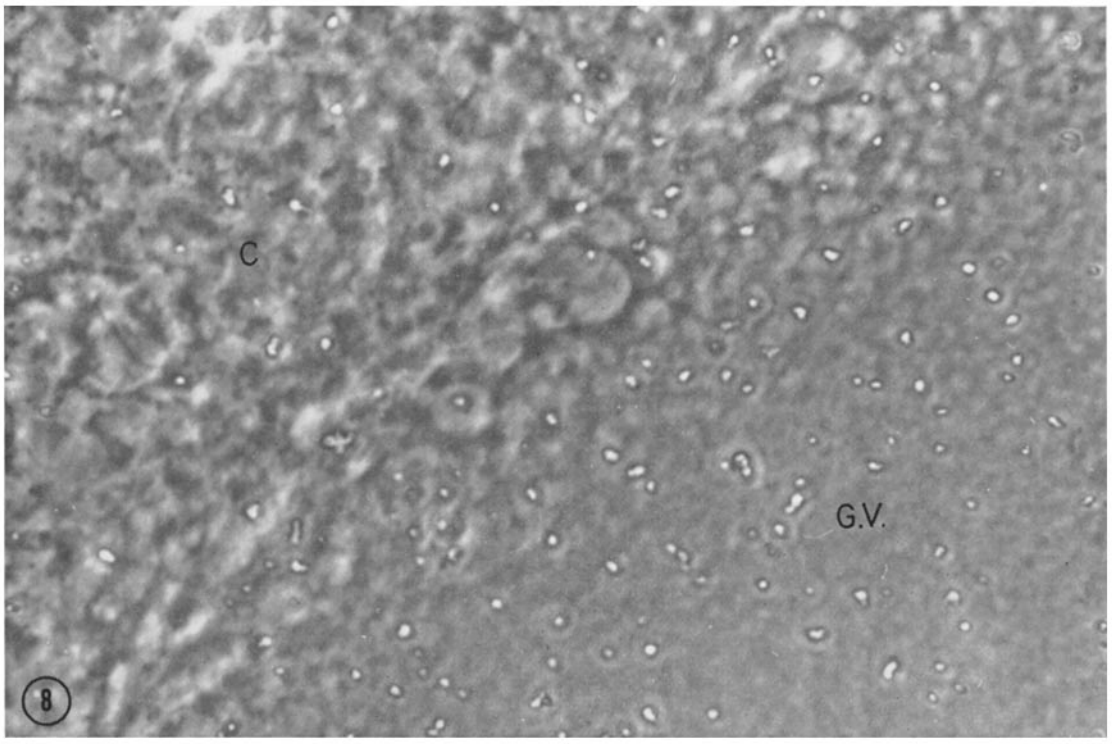

FIGURE 8. Phase contrast view of a radioautograph of the germinal vesicle (*G.V.*)–cytoplasm (*C*) border at t_E = 260 sec. × 1800.

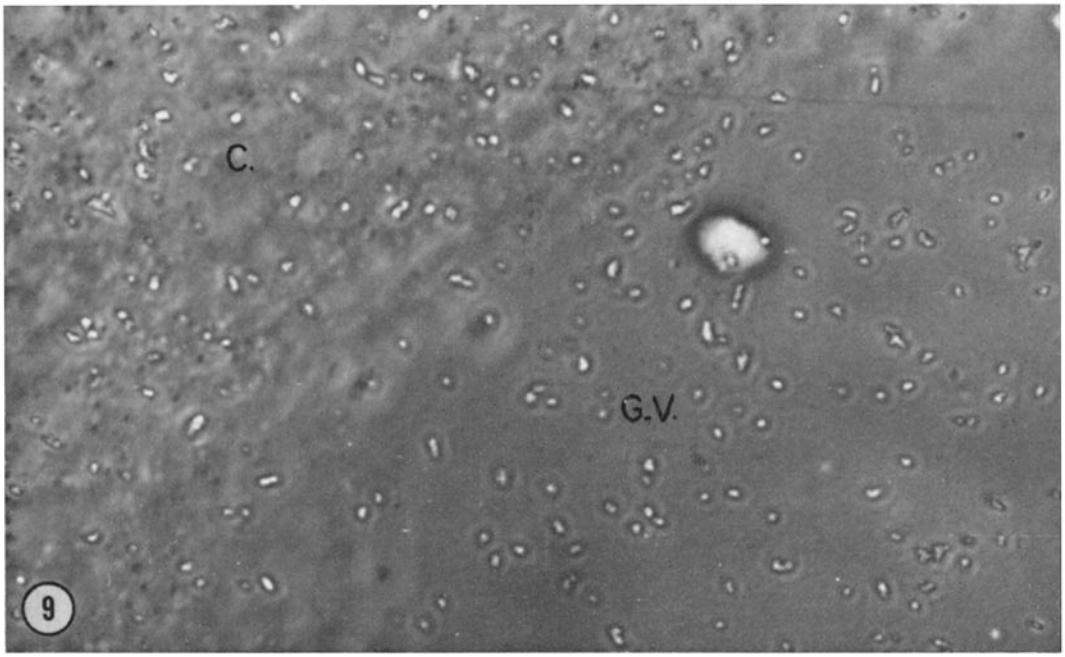

FIGURE 9. Phase contrast view of a radioautograph of the germinal vesicle (*G.V.*)–cytoplasm (*C*) border at t_E = 8890 sec. × 1800.

In general both germinal vesicle and animal hemisphere cytoplasm show greater regional variation in grain density than vegetal hemisphere sections. This is especially true of the germinal vesicle where variation seems largely attributable to the influence of the type 2 artifact. However, the conclusion one draws from the examination of large numbers of germinal vesicles is that,

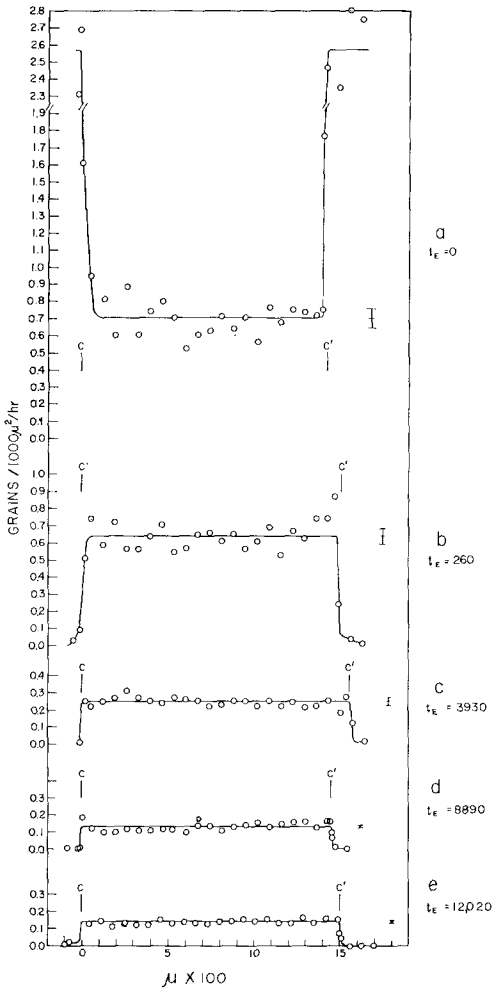

FIGURE 10. Grain density profiles through the cytoplasm of oocytes equilibrated with glycerol-^{3}H Ringer's solution at (a) equilibrium (frozen and sectioned in AG*-Ringer's), and (b–e) washed out for various t_E (as indicated) (frozen and sectioned in AG-Ringer's). C and C' are oocyte boundaries. For additional explanation see text.

barring artifacts, the distribution of activity in the germinal vesicle is uniform, at all values of t_E, within the limits of resolution of the method.

In most profiles, a sharp discontinuity is seen exactly at the border of the germinal vesicle. However, this is by no means universal and high grain counts are often observed in the perinuclear region. The most usual case is one in which part of the vesicle circumference coincides exactly with a sharp

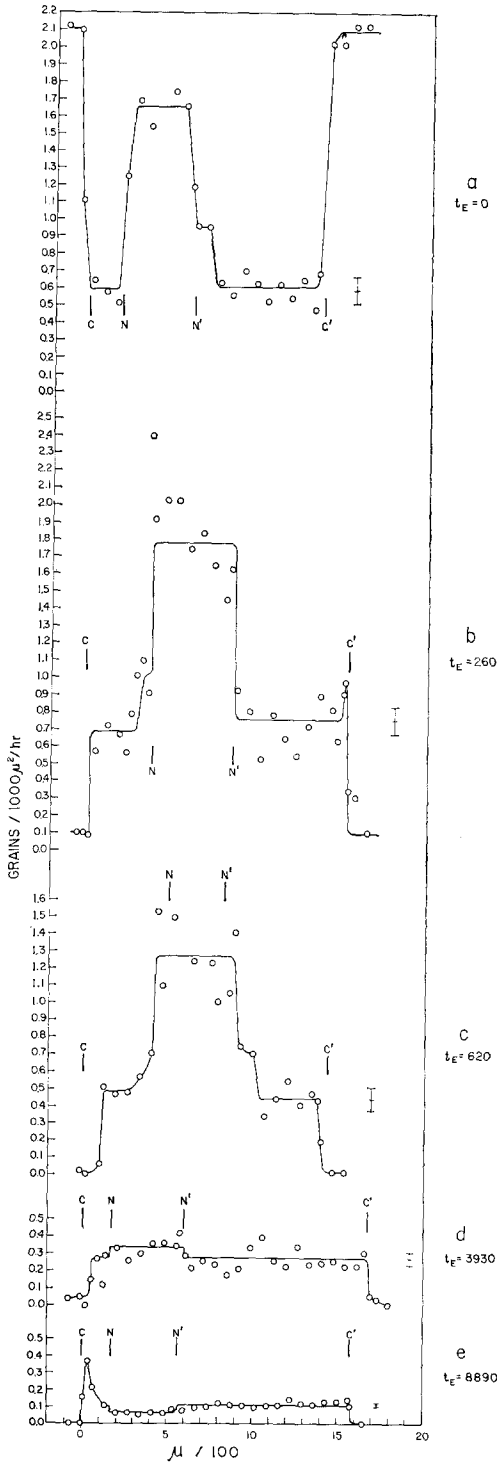

FIGURE 11. Grain density profiles through the animal hemisphere of oocytes equilibrated with glycerol-^3H Ringer's solution at (a) equilibrium, $t_E = 0$ (frozen and sectioned in AG*-Ringer's), and (b–e) washed out for various t_E (as indicated) (frozen and sectioned in AG-Ringer's). C and C' are oocyte boundaries, N and N' are germinal vesicle boundaries. For additional explanation see text.

discontinuity in the grain count profile while at other parts high grain counts extend into surrounding cytoplasm. In our preparations no histological difference is seen between high and low count perinuclear regions, but the development and bleaching treatments alter the oocyte sections sufficiently to make this observation quite inconclusive.

At equilibrium (Fig. 11 a) the grain density in the germinal vesicle is considerably higher than in the cytoplasm. With increasing t_E (Fig. 11 b–e) the activity in the germinal vesicle falls, and for large values of t_E is actually less than the activity in the cytoplasm; this can be seen in Figs. 9 and 11 e.

The mean grain densities in the cytoplasm, G_c, and in the germinal vesicle, G_n, are plotted in Fig. 12 as a function of t_E. In each compartment there is

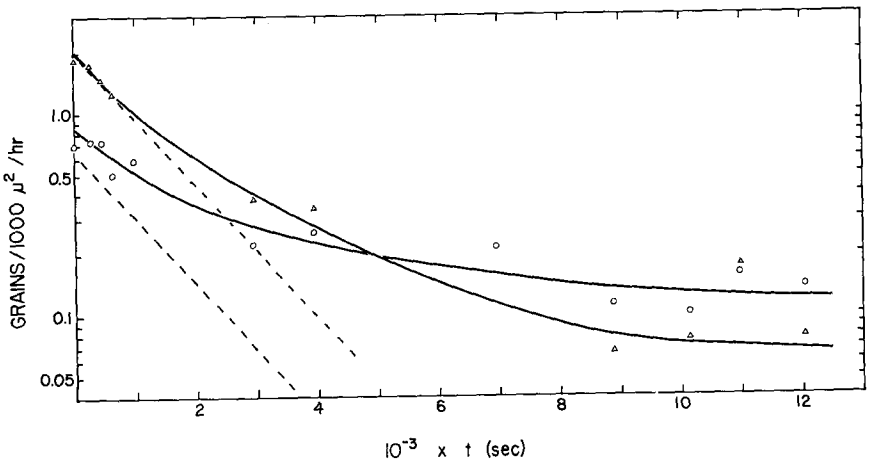

FIGURE 12. Mean grain density, as determined by radioautography, in germinal vesicle (triangles) and cytoplasm (circles) of oocytes as a function of t_E at 13.6°C. Points experimental, lines fitted. Dashed lines are the fast fraction component of the solid lines. See text for additional explanation.

both a fast and slow fraction, but the amount of each fraction is different in each. The nuclear and cytoplasmic fast fractions, indicated by dashed lines, have identical rate constants of 7.4×10^{-4} sec $^{-1}$, in good agreement with the value of 7.7×10^{-4} sec^{-1} determined by extraction. No attempt has been made to fit two terms to the slow fractions because of the considerable scatter of the data. The approximate single exponential rate constants for the slow fractions in both compartments are 4×10^{-5} sec^{-1} which does not differ significantly from that for a single exponential term fitted to the two terms of the slow fraction determined by extraction (Fig. 5).

Quantitation

The grain density beneath sections of AG*-Ringer's was 1.93 ± 0.07 grains/1000 μ^2/hr. This derives from a source of activity 0.339 mc/cm^3 in the liquid

state; assuming the volume expansion on freezing to be given by the normal expansion of the water in the solution, a volume increase of 7.7% can be calculated, giving an activity in the frozen section of 0.315 mc/cm^3. The ratio of grain density to activity is therefore 1.93/0.315 = 6.13. The corresponding figure for the polymer standard is 9.91/density = 9.91/1.06 = 9.35. The efficiency with AG*-Ringer's is therefore 34% smaller than with the polymer. The reasons for this are not yet clear, and are currently being studied. A strong possibility is that, as ice crystals are frozen out of the solution, glycerol-^3H is concentrated into intercrystalline regions rich in protein and salts. The electron opacity of these regions is greater than that of the polymer, so that more absorption of emitted electrons will occur; also, since the range of tritium electrons is very small, concentration of the emitters into a small volume will in-

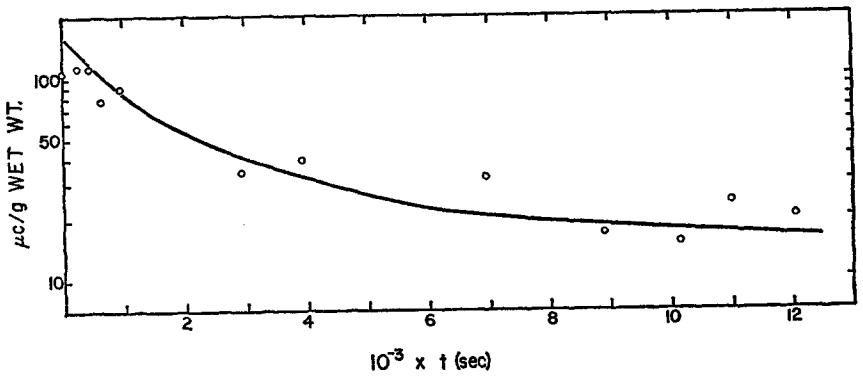

FIGURE 13. Oocyte concentration of glycerol-^3H as determined by extractive analysis (line) and radioautographic analysis (points). The line is the same as in Fig. 5. AG*-Ringer's used as standard. For additional explanation see text.

crease the probability of multiple hits on the emulsion grains, increasing the correction above that given in Fig. 3.

If an explanation of this sort is correct, the AG*-Ringer would be expected to be a better standard than the polymer for quantitation of the oocyte radioautographs. A test of this can be obtained by attempting to recover the quantitative features of the efflux, as determined by extraction (Fig. 5), using the radioautographic efflux curves (Fig. 12) and the AG*-Ringer as a standard. This has been done in Fig. 13. If $G_n(t_E)$ and $G_c(t_E)$ are the grain densities in the germinal vesicle and cytoplasm, respectively, at time t_E, and W_n and W_c the fractional weights of the compartments, the mean cellular activity in millicuries per gram is given by

$$\bar{C}'(t_E) = \frac{W_n G_n(t_E) + 0.974 W_c G_c(t_E)}{6.50}.$$

The factor 6.50 is derived from the AG*-Ringer calibration figure, 6.13, times

315/339 to convert to the liquid volume, times the mean tissue density of 1.14 to convert to activity per gram. The factor 0.974 accounts for the smaller volume change on freezing of the cytoplasm, which is only 50% water. The difference in density between cytoplasm and germinal vesicle has been omitted, as it gives a negligible correction.

The points in Fig. 13 are calculated in this manner from the radioautographic data, and the solid line is taken from Fig. 5. The agreement is quite good, and would obviously have been considerably poorer if the polymer had been used as the standard. The points tend to be about 20% low at small t_E and about 5% high at large t_E. This is not unexpected, in view of the behavior of AG*-Ringer's and the higher density of oocyte cytoplasm: at activities comparable to that in the AG*-Ringers the efficiency would be ex-

TABLE I

GLYCEROL FRACTIONS IN THE OOCYTE DETERMINED BY EXTRACTION AND BY RADIOAUTOGRAPHY

	Fast			Slow		
	μc/g wet wt.	*μc/ml H_2O*	*space*	*μc/g wet wt.*	*μc/ml H_2O*	*space*
Cytoplasm (extractive)	123	246	0.73	30	60	0.18
Cytoplasm	97 (107)	194 (214)	0.57 (0.63)	31	62	0.18
Germinal vesicle	288	327	0.96	12	14	0.04

Slow and zero-rate fractions are not distinguished. Space is calculated as the ratio of μc/ml H_2O to the value in the incubation medium, 339 μc/ml. The extractive estimate of the cytoplasmic fractions was obtained by subtracting from the total extractive data (equation 1) approximate nuclear contributions based on a fractional nuclear volume of 0.024 and water content of 0.88 ml/g, and taking the nuclear solvent spaces to be 1.0 for the fast fraction and 0.04 for the slow.

pected to be lower in the more dense medium, whereas at low activities the excess multihit error, anticipated in AG*-Ringer's, would be ameliorated. An additional factor is likely to be operative, as follows.

In radioautographs of oocyte cytoplasm, particularly in the vegetal hemisphere, the silver grains tend to occur in a reticulate pattern with interspaces of a size and shape appropriate to the yolk platelets (cf. Fig. 1 b and Fig. 6 b). This appears to reflect the distribution of glycerol-^{3}H in the cytoplasmic water between the platelets and possibly binding on the periphery of the platelets. The standard counting square (69 μ × 69 μ) is large enough to include numerous platelets as well as interspaces, and the grain count in a square is a weighted average of high and low activity areas. The multiple hit correction is based on this weighted average. It would be more precise to base the correction on the true interplatelet grain density. This is, however, not possible and as a result the multihit correction used for high density radioautographs

of oocyte cytoplasm is regularly too small. The effect is difficult to estimate, but a rough calculation suggests that the correction would boost cytoplasmic densities at small values of t_E by about 10%. This would reduce the maximum difference between the two curves to about 15%.

Again using the AG*-Ringer standard, the amounts of each fraction in each compartment may be estimated from the data of Fig. 12. The slow and "zero-rate" fractions are not distinguished. The values obtained are given in Table I, together with values estimated for the cytoplasm from the extractive data by subtracting a small estimated nuclear contribution of 3.1% from the fast fraction and 1.7% from the slow fraction. The values in parentheses have been increased by 10% to show the effect of the correction mentioned above. The values designated "space" are derived by dividing the activity in μc/ml H_2O by 339 μc/ml, the activity of G*-Ringer's, and represent the effective fraction of the water in each compartment which is acting as a solvent for the particular glycerol fraction. The water contents of the compartments were taken as: cytoplasm, 0.5 ml/g; germinal vesicle, 0.88 ml/g (6).

DISCUSSION

We can designate four fractions of glycerol in the oocyte: the cytoplasmic fast (CF) and slow (CS) fractions, and the nuclear fast (NF) and slow (NS) fractions. The interpretation of these will be considered in turn.

The CF fraction represents the major portion of the cytoplasmic glycerol, and is uniformly distributed throughout the cytoplasm up to the cell surface. We infer that this fraction is freely diffusible glycerol, whose efflux from the cell is determined by permeation through the cortical membrane. The membrane permeability P, calculated from the rate constant of 7.7×10^{-4} sec^{-1}, is 2.2×10^{-5} cm/sec. This is appreciably larger (Table II) than values reported for glycerol in other cells. However, the oocyte cortex is highly microvillous, so that its effective surface is substantially greater than the surface apparent in light microscopy. In young oocytes the surface area is about 35 times the surface area of a simple sphere (13). If a comparable ratio prevails in the Y_5 oocyte, the true permeability would compare well with the values in other cells.

The rate of diffusion of the CF fraction within the cytoplasm cannot be directly evaluated, since no diffusional profile is seen. Detailed analysis, published elsewhere (11), shows that, for the diffusional contribution to the flux rate to be negligible, the diffusion coefficient of glycerol in the cytoplasm must be no smaller than about 1.7×10^{-6} cm^2/sec, a value ≥ 0.24 times that of glycerol in dilute aqueous solution. This ratio is similar to the values of ≤ 0.26 estimated by Løvtrup (32) and 0.30–0.60 estimated by Ling et al. (9) for the ratio of the diffusion coefficients of tracer water in the oocyte and free solution, indicating that there is little molecular sieving of small molecules by the cyto-

plasm. The contrast between the flux of water, which Løvtrup (32) and Ling et al. (9) have inferred is diffusion-limited, and that of glycerol, which in the present study is clearly membrane-limited, arises from the much smaller permeability of the membrane to glycerol than to water (see also reference 11).

The solvent space accessible to the CF fraction is no more than 73% of the water of the cytoplasm (Table I), even though more than ample time for influx equilibration of this fraction was allowed during incubation. As will be described below, the same is not true of the germinal vesicle: essentially all of the nuclear water is accessible to freely diffusing glycerol. Part of the inaccessible cytoplasmic water may be within yolk platelets, since the radioautographs suggest that glycerol is, at least partially, excluded from the platelets

TABLE II

PERMEABILITY COEFFICIENTS FOR GLYCEROL DETERMINED BY ISOTOPIC OR CHEMICAL METHODS

	T	P
	°C	$cm/sec \times 10^7$
Chara (28)	18–23	2.1
Frog sartorius*	13.6	3.5
Toad bladder (30)	25	4.1
Squid axon (31)	22–24	26
Frog oocyte (fast fraction)	13.6	218‡

* Unpublished results, for method see (29).

‡ Assuming a smooth surface, see text.

(see page 722); or the water may be slowly accessible, and be associated with the CS fraction; this will be discussed further below.

The CS fraction represents glycerol in the cytoplasm whose rate of efflux is at least 10 times slower than would be given by the membrane permeability. This glycerol is therefore taken to be bound to one or more impermeant cytoplasmic constituents. Radioautography at 14 μ resolution indicates only that these constituents are uniformly distributed in the cytoplasm outside, probably, of the yolk platelets, as in the case of the CF fraction. Whether the constituents are soluble macromolecules, particles, or vesicles, small relative to the resolution, cannot be stated. While on occasion it has been suggested (33–35) that specific glycerol-binding sites occur in membranes, the present binding need not be specific: either membrane-enclosed cytoplasmic vesicles of low permeability, such as suggested by Merriam (10) to account for the osmotic properties of surface-damaged oocytes, or polar binding to macromolecules, such as is seen in keratin fibers (36), may be involved. There is no conclusive evidence to indicate whether the glycerol CS fraction may be associated with the cytoplasmic water which is not acting as a solvent for the CF fraction; a slow fraction of tracer water flux as large as 0.25 of the total

oocyte water has been reported by Ling et al. (9), but this is quite variable in amount.

The kinetics of efflux of the CS fraction may be interpreted as follows. We assume that bound glycerol may dissociate from its binding constituent to become freely diffusible and able to pass through the cortical membrane; similarly, freely diffusible glycerol in the cytoplasm may become bound. Since chemical equilibrium at $t_E = 0$ between diffusible and bound glycerol may be assumed (except possibly for the small zero-rate fraction, C_∞, in equation 1), the binding of tracer is pseudo-first order, and we may write schematically

$$\text{CS} \underset{k_2}{\overset{k_1}{\rightleftharpoons}} \text{CF} \xrightarrow{k_m} \text{out}$$

In the present case, we have $k_m = k_f = 7.7 \times 10^{-4}$ sec $^{-1}$, $k_1 = k_s = 8.8 \times 10^{-5}$ sec^{-1}, and $k_2 \cong \frac{0.18}{0.73} k_1$ (Table I) $= 2.2 \times 10^{-5}$ sec^{-1}. As is implicit in the kinetic analysis, the two fractions are kinetically independent because of the great difference between k_m and k_1. Physically, the CF fraction leaves the cell before any substantial change in the CS fraction; during subsequent efflux of CS, a quasi–steady-state concentration of CF is maintained at a value of approximately (k_1/k_m)[CS] ≈ 0.11 [CS]. The above reaction scheme proceeds essentially unidirectionally from left to right during efflux.

The NF fraction represents 96% of the nuclear glycerol. It is uniformly distributed in the germinal vesicle, and its space is virtually identical to the water space in amount. The rate constant for efflux of the NF fraction is identical to that for the CF fraction. We infer the following. (*a*) The NF fraction is freely diffusible glycerol distributed passively in the nuclear water. (*b*) The nuclear membrane is a negligible barrier to the diffusion of glycerol; the NF and CF fractions are in diffusional equilibrium with each other during efflux, so that for both, the rate constant for loss from the cell is determined by the permeability of the cortical membrane. (*c*) There is no evidence for a significant independent diffusional pathway from the germinal vesicle to the exterior not requiring passage of glycerol molecules through the cytoplasm; this is in agreement with the absence of such channels in electron micrographs, and with the inference of Naora et al. (6) based on flux studies using ^{22}Na. Schematically, we have:

$$\text{NF} \underset{k_4}{\overset{k_3}{\rightleftharpoons}} \text{CF} \xrightarrow{k_m} \text{out}$$

with $k_m \ll k_3, k_4$.

The permeability of the nuclear membrane of amphibian oocytes has been

the subject of considerable study. In general germinal vesicles have been found to be very permeable to small molecules when studied as isolated preparations or osmotically *in situ* (37–41). Kanno and Loewenstein (42) found a negligible membrane resistance and no potential in germinal vesicles *in situ* in immature (up to 350 μ) *Xenopus* oocytes; however, Morrill and Watson (43) have reported that the germinal vesicle in mature *Rana pipiens* oocytes is about 26 mv positive to the cytoplasm. The Na^+ and K^+ concentrations, in microequivalents per milliliter of H_2O, are much higher in the germinal vesicle than in the cytoplasm, ratios of 3.2:1 and 2.4:1, respectively, having been found by Naora et al. (6). However, there appears to be only a slight delay in the rate of specific labeling with ^{22}Na of readily exchangeable nuclear Na^+, relative to cytoplasmic, indicating again, as do the present results, a high nuclear membrane permeability.

The NS fraction is quite small; per milliliter of compartment water, NS is only 23% as large as CS. The fraction is uniformly distributed within the germinal vesicle and is not, for example, associated with the centrally located chromosomal frame and nucleolar cloud which is present in mature germinal vesicles (44). The same reasoning that was applied to the CS fraction leads to the inference that the NS fraction is bound to impermeant nuclear constituents, and that its flux from the cell is determined by the rate of dissociation from the binding constituent. This inference is not as secure as that pertaining to the CS fraction, because the NS fraction is below the resolution of the chromatographic techniques, so that a positive identification as glycerol is not possible.

In either case, the distribution of glycerol-binding constituents is not uniform between the cytoplasm and the germinal vesicle, there being more in the cytoplasm. The binding constituents need not be chemically identical in the two compartments; while the flux rate constants for NS and CS are similar (Fig. 12), there is considerable latitude in estimating the exact values.

There are few, if any, membrane-bounded microvesicular structures within the nucleus so that the NS fraction is not of microvesicular origin. Such structures are, however, abundant in the cytoplasm, and as mentioned earlier cannot be excluded in considering the origin of the CS fraction.

The kinetic scheme for efflux of the NS fraction is similar to that for the CS, except that the former becomes freely diffusible within the germinal vesicle before passing into the cytoplasm:

$$\mathrm{NS} \underset{k_6}{\overset{k_5}{\rightleftharpoons}} \mathrm{NF} \underset{k_4}{\overset{k_3}{\rightleftharpoons}} \mathrm{CF} \xrightarrow{k_m} \mathrm{out}$$

As before, $k_6 < k_s \approx k_5 < k_m = k_f \ll k_3, k_4$.

As in the case of the cytoplasmic fractions, NF leaves the cell almost completely before any appreciable change in NS. This independence of fast and slow fractions, together with the fact that CS is larger than NS, accounts for the fall of G_n below G_c in Fig. 12 without the need to invoke separate channels from germinal vesicle to exterior.

Sodium transport in the mature frog oocyte bears marked resemblances to that of glycerol and reflects on the generality of the conclusions drawn here. As in the case of glycerol, four fractions can be designated: Na_{CF}, Na_{CS}, Na_{NF}, and Na_{NS}. The flux of the total fast fraction at 20°C is exponential and has a rate constant of 6.6×10^{-4} sec^{-1} (determined from (5) Fig. 4); for the slow fraction the rate constant is about 4×10^{-5} sec^{-1} (determined from (5) Fig. 3). These are quite similar to those of glycerol. Furthermore, the values for the rate constants for Na_{CF} and Na_{NF}, and Na_{CS} and Na_{NS} appear to be similar (6). The ratio of the concentrations of Na in the water of the germinal vesicle and cytoplasm is 3.2:1; the relative concentrations of fast and slow fractions in the two compartments (Na_{CF}:Na_{CS} and Na_{NF}:Na_{NS}) are the same, about 1:5.7 (6). The concentration of Na_{CF} in the cytoplasmic water is only about 0.11 that of Na in Ringer's solution. It is likely that, like fast fraction glycerol, Na_{CF} is in free solution; its exclusion from the cell is presumably attributable to a sodium pump. The very large Na slow fraction appears to be bound, a conclusion consistent with recent NMR and cation-sensitive glass electrode studies, which indicate the existence of large bound Na fractions in other tissues (45–49). The uniformity of the ratios of fast to slow Na fractions in cytoplasm and nucleus indicates that the concentration of Na binding sites is the same in nuclear and cytoplasmic water. This suggests that slow fraction Na is not held in microvesicular structures. The question of the relationship of Na binding structures to those that bind glycerol is an interesting, but at present, unanswered one.

In viewing the purely technical aspects of the work, we can conclude that quantitative solute radioautography is a useful tool. However, improvements in the technique will be necessary to enhance the generality of its usefulness. In particular, resolution must be increased before the method can be profitably applied to cells of conventional size. Also the factors affecting quantitation of frozen-section radioautographs must be elucidated in detail, so as to be controllable. An improvement in technique that holds promise for improved resolution is a substantial reduction in cutting temperatures. There is actually an improvement in tissue-cutting properties at very low temperatures, and ultrathin sections are achieved (50, 51), raising the prospect of reducing resolution loss attributable to β-particle scatter.

The authors are indebted to Professor William Kinter for his generous help in the initial stages of this study.

This study was supported in part by United States Public Health research grant (GM 11070) from the Institute of General Medical Sciences, United States Public Health Service, and National Science Foundation research grant GB 5825.

Received for publication 29 September 1967.

REFERENCES CITED

1. OSTER, H., H-W. KUNDT, and R. TAUGNER. 1955. Methodische Untersuchungen zur autoradiographischen Darstellung wasserlöslicher Stoffe in der Niere. *Arch. Exptl. Path. Pharmakol.* **224**:476.
2. APPLETON, T. C. 1964. Autoradiography of soluble labelled compounds. *J. Roy. Microscop. Soc.* **83**:277.
3. KINTER, W. B., and T. H. WILSON. 1965. Autoradiographic study of sugar and amino acid absorption by everted sacs of hamster intestine. *J. Cell Biol.* **25**:19.
4. MORRILL, G. A., J. ROSENTHAL, and D. E. WATSON. 1966. Membrane permeability changes in amphibian eggs at ovulation. *J. Cellular Physiol.* **67**:375.
5. ABELSON, P. H., and W. R. DURYEE. 1949. Radioactive sodium permeability and exchange in frog eggs. *Biol. Bull.* **96**:205.
6. NAORA, H., H. NAORA, M. IZAWA, V. G. ALLFREY, and A. E. MIRSKY. 1962. Some observations on differences in composition between the nucleus and cytoplasm of the frog oöcyte. *Proc. Natl. Acad. Sci.* **48**:853.
7. MORRILL, G. A. 1966. Water and electrolyte changes in amphibian eggs at ovulation. *Exptl. Cell Res.* **40**:664.
8. MERRIAM, R. W. 1966. Some characteristics of amino acid transport in frog ovarian oöcytes. *Exptl. Cell Res.* **42**:340.
9. LING, G. N., M. M. OCHSENFELD, and G. KARREMAN. 1967. Is the cell membrane a universal rate-limiting barrier to the movement of water between the living cell and its surrounding medium? *J. Gen. Physiol.* **50**:1807.
10. MERRIAM, R. W. 1966. The role of cytoplasmic membranes in the regulation of water concentration within frog oöcytes. *Exptl. Cell Res.* **41**:34.
11. FENICHEL, I. R., and S. B. HOROWITZ. 1968. Intracellular transport. *In* Biological Membranes. R. M. Dowben, editor. Little, Brown and Co., Boston. In press.
12. KEMP, N. E. 1953. Synthesis of yolk in oöcytes of *Rana pipiens* after induced ovulation. *J. Morphol.* **92**:487.
13. KEMP, N. E. 1956. Electron microscopy of growing oocytes of *Rana pipiens*. *J. Biophys. Biochem. Cytol.* **2**:281.
14. WARTENBERG, H., and W. SCHMIDT. 1961. Elektronenmikroskopische Untersuchungen der strukturellen Veränderungen im Rindenbereich des Amphibieneies im Ovar und nach der Befruchtung. *Z. Zellforsch. Mikroskop. Anat.* **54**:118.
15. WARTENBERG, H. 1962. Elektronenmikroskopische und histochemische Studien über die Oogenese der Amphibieneizelle. *Z. Zellforsch. Mikroskop. Anat.* **58**:427.
16. KEMP, N. E., and N. L. ISTOCK. 1967. Cortical changes in growing oöcytes and in fertilized or pricked eggs of *Rana pipiens*. *J. Cell Biol.* **34**:111.
17. BRAY, G. A. 1960. A simple efficient liquid scintillator for counting aqueous solutions in a liquid scintillation counter. *Anal. Biochem.* **1**:279.
18. BANDURSKI, R. S., and B. AXELROD. 1951. The chromatographic identification of some biologically important phosphate esters. *J. Biol. Chem.* **193**:405.
19. CHARGAFF, E., C. LEVINE, and C. GREEN. 1948. Techniques for the demonstration by chromatography of nitrogenous lipid constituents, sulfur-containing amino acids, and reducing sugars. *J. Biol. Chem.* **175**:65.
20. KINTER, W. B., L. L. LEAPE, and J. J. COHEN. 1960. Autoradiographic study of Diodrast-I^{131} transport in *Necturus* kidney. *Am. J. Physiol.* **199**:931.
21. COONS, A. H., E. H. LEDUC, and M. H. KAPLAN. 1951. Localization of antigen in tissue cells. IV. The fate of injected foreign proteins in the mouse. *J. Exptl. Med.* **93**:173.

22. RITZEN, M. 1967. A method for the autoradiographic determination of absolute specific radioactivity in cells. *Exptl. Cell Res.* **45**:250.
23. HILL, D. K. 1962. Resolving power with tritium autoradiographs. *Nature.* **194**:831.
24. LEBLOND, C. P., B. KOPRIWA, and B. MESSIER. 1963. Radioautography as a histochemical tool. 1st International Congress Histochemistry and Cytochemistry, Paris. Pergamon Press, Oxford. 1.
25. MOORE, A. C. 1951. The effect of pressure and friction on photographic emulsions. *Brit. J. Appl. Phys.* **2**:20.
26. BOYD, G. A. 1955. Autoradiography in Biology and Medicine. Academic Press, Inc., New York. 145.
27. LELOIR, L. F., and C. F. CARDINI. 1957. Characterization of phosphorus compounds by acid lability. *In* Methods in Enzymology. S. P. Colowick and N. O. Kaplan, editors. Academic Press, Inc., New York. **3**:840.
28. COLLANDER, R., and H. BARLUND. 1933. Permeabilitätsstudien an *Chara ceratophylla.* II. Die Permeabilität fur Nichtelektrolyte. *Acta Botan. Fenn.* **11**:5.
29. FENICHEL, I. R., and S. B. HOROWITZ. 1963. The transport of non-electrolytes in muscle as a diffusional process in cytoplasm. *Acta Physiol. Scand.* **60** (Suppl. 221):1.
30. LEAF, A., and R. M. HAYS. 1962. Permeability of the isolated toad bladder to solutes and its modification by vasopressin. *J. Gen. Physiol.* **45**:921.
31. VILLEGAS, R., C. CAPUTO, and L. VILLEGAS. 1963. Diffusion barriers in the squid nerve fiber. The axolemma and the Schwann layer. *J. Gen. Physiol.* **46**:245.
32. LØVTRUP, S. 1963. On the rate of water exchange across the surface of animal cells. *J. Theoret. Biol.* **5**:341.
33. LEFEVRE, P. G. 1948. Evidence of active transfer of certain non-electrolytes across the human red cell membrane. *J. Gen. Physiol.* **31**:505.
34. WIDDAS, W. F. 1954. Facilitated transfer of hexoses across human erythrocyte membrane. *J. Physiol., (London).* **125**:163.
35. STEIN, W. D. 1962. Spontaneous and enzyme-induced dimer formation and its role in membrane permeability. *Biochim. Biophys. Acta.* **59**:47.
36. HOROWITZ, S. B., and I. R. FENICHEL. 1966. Transport and solubility in hydrated keratin. *In* Membranes and Transport Phenomena. Biophysical Society 10th Annual Meeting. Boston, Massachusetts.
37. CALLAN, H. G. 1952. A general account of experimental work on amphibian oöcyte nuclei. *Symp. Soc. Exptl. Biol.* **6**:243.
38. BATTIN, W. T. 1959. The osmotic properties of nuclei isolated from amphibian oöcytes. *Exptl. Cell Res.* **17**:59.
39. HARDING, C. V., and C. FELDHERR. 1959. Semipermeability of the nuclear membrane in the intact cell. *J. Gen. Physiol.* **42**:1155.
40. HUNTER, A. S., and F. R. HUNTER. 1961. Studies of volume changes in the isolated amphibian germinal vesicle. *Exptl. Cell Res.* **22**:609.
41. MACGREGOR, H. C. 1962. The behavior of isolated nuclei. *Exptl. Cell Res.* **26**:520.
42. KANNO, Y., and W. R. LOEWENSTEIN. 1963. A study of the nucleus and cell membranes of oocytes with an intra-cellular electrode. *Exptl. Cell Res.* **31**:149.
43. MORRILL, G. A., and D. E. WATSON. 1966. Transmembrane electropotential changes in amphibian eggs at ovulation, activation and first cleavage. *J. Cellular Physiol.* **67**:85.
44. DURYEE, W. R. 1950. Chromosomal physiology in relation to nuclear structure. *Ann. N.Y. Acad. Sci.* **50**:920.
45. HINKE, J. A. M. 1961. The measurement of sodium and potassium activities in the squid axon by means of cation-selective glass micro-electrodes. *J. Physiol., (London).* **156**:314.
46. LEV, A. A. 1964. Determination of activity and activity coefficients of potassium and sodium ions in frog muscle fibres. *Nature.* **201**:1132.
47. MCLAUGHLIN, S. G. A., and J. A. M. HINKE. 1966. Sodium and water binding in single striated muscle fibers of the giant barnacle. *Can. J. Physiol. Pharmacol.* **44**:837.
48. COPE, F. W. 1967. NMR evidence for complexing of Na^+ in muscle, kidney, and brain,

and by actomyosin. The relation of cellular complexing of Na^+ to water structure and to transport kinetics. *J. Gen. Physiol.* **50**:1353.

49. ROTUNNO, C. A., V. KOWALEWSKI, and M. CEREIJIDO. 1967. Nuclear spin resonance evidence for complexing of sodium in frog skin. *Biochim. Biophys. Acta.* **135**:170.
50. STUMPF, W. E., and L. J. ROTH. 1965. Frozen sectioning below −60°C with a refrigerated microtome. *Cryobiology.* **1**:227.
51. CHRISTENSEN, A. K. 1967. A simple way to cut frozen thin sections of tissue at liquid nitrogen temperatures. *Anat. Rec.* **157**:227. (Abstr.)